

Superconductivity in the YIr_2Si_2 and LaIr_2Si_2 Polymorphs

Michal Vališka, Jiří Pospíšil, Jan Prokleška, Martin Diviš, Alexandra Rudajevová, and Vladimír Sechovský
*Faculty of Mathematics and Physics, Charles University,
 DCMF, Ke Karlovu 5, CZ-12116 Praha 2, Czech Republic*

We report on existence of superconductivity in YIr_2Si_2 and LaIr_2Si_2 compounds in relation to crystal structure. The two compounds crystallize in two structural polymorphs, both tetragonal. The high temperature polymorph (HTP) adopts the CaBe_2Ge_2 -structure type (space group $P4/nmm$) while the low temperature polymorph (LTP) is of the ThCr_2Si_2 type ($I4/mmm$). By studying polycrystals prepared by arc melting we have observed that the rapidly cooled samples retain the HTP even at room temperature (RT) and below. Annealing such samples at $\geq 900^\circ\text{C}$ followed by slow cooling to RT provides the LTP. Both, the HTP and LTP were subsequently studied with respect to magnetism and superconductivity by electrical resistivity, magnetization, AC susceptibility and specific heat measurements. The HTP and LTP of both compounds respectively, behave as Pauli paramagnets. Superconductivity has been found exclusively in the HTP of both compounds below T_{SC} ($= 2.52\text{ K}$ in YIr_2Si_2 and 1.24 K in LaIr_2Si_2). The relations of magnetism and superconductivity with the electronic and crystal structure are discussed with comparing experimental data with the results of first principles electronic structure calculations.

Keywords: YIr_2Si_2 , LaIr_2Si_2 , superconductivity, polymorphism, electronic structure calculations

I. INTRODUCTION

To date large variety of ternary intermetallic systems has been discovered and many of them remain subjects of intensive scientific interest. The rare-earth intermetallics are the most intensively studied with respect to the cooperative phenomena – magnetism and superconductivity. The localized $4f$ electrons of the rare-earth ions exposed to various crystallographic and chemical environments in compounds cause a rich spectrum of the physical phenomena like magnetism with various magnetic structures, heavy fermion behavior or unconventional superconductivity in the quantum critical regime. The weak interactions of localized $4f$ electrons with valence electrons of neighboring ions, which are the key ingredients of the physics of these intermetallics, are strongly dependent on the complex interplay of chemistry and symmetry of the neighborhood. Studies of La, Lu or Y analogues allow inspecting properties independent on presence of $4f$ -electrons in the material.

Only in some specific cases one can investigate the effect of crystal symmetry change alone without changing composition. An outstanding opportunity is offered by polymorphism. Polymorphism is a unique phenomenon when the material can appear in two or even few different crystal structures although the chemical stoichiometry and composition are conserved. It means that the same collection of ions can be arranged to two or more crystal structures of different symmetry.

One large group of materials exhibiting often polymorphism is characterized by the composition $RE\text{T}_2\text{X}_2$, where RE represents various rare-earth ions, T stays for $3d$, $4d$ and $5d$ transition metals and noble metals, e.g. Ag or Au and X represents p -elements like Si, Ge, As or P^{1–14}. Two polymorphs can be found in the case of 122 iridium silicides. One polymorph crystallizes in the primitive tetragonal structure of the

CaBe_2Ge_2 type (space group $P4/nmm$) and the second adopts the ThCr_2Si_2 -type body centered tetragonal structure ($I4/mmm$). The ThCr_2Si_2 -type is thermodynamically stable at room temperature (LTP) while the CaBe_2Ge_2 -type is thermodynamically stable at high temperatures (HTP). Nevertheless, the HTP can exist as a metastable form at room temperature when the cooling rate from the melt is high enough. The temperatures of the structural transitions between polymorphs are the characteristic parameters of each polymorphic compound. Existence of the polymorphism is probably not the general rule in the entire group of the $RE\text{Ir}_2\text{Si}_2$ compounds. For example EuIr_2Si_2 is reported crystallizing only in the CaBe_2Ge_2 -type structure^{4,15}.

The group of 122 rare-earth-iridium silicides exhibits variety of phenomena like magnetism, superconductivity or non-Fermi liquid behavior. A short overview is presented in the following paragraph together with motivation of our work.

The Ce analogue does not order magnetically, neither the HTP nor the LTP variant presumably due to lack of Ce magnetic moments of valence fluctuating Ce ions. The LTP behaves as the Fermi-liquid at low temperatures whereas the HTP exhibits non-Fermi-liquid features^{16,17}. It is in contrast to the uranium polymorphs, which order antiferromagnetically in the LTP whereas the HTP is paramagnetic at low temperatures^{1,12,18}.

Similar situation to U compounds has been found in the Pr polymorphs. The HTP is paramagnetic down to 2 K while the LTP orders antiferromagnetically at $T_{\text{N}} = 45.5\text{ K}$. Magnetism of the Pr polymorphs is determined by the crystal field (CF) acting on the Pr ion^{19–22}. The Nd compounds behave likewise the Pr ones. The HTP is entirely paramagnetic whereas the LTP becomes antiferromagnetic below $T_{\text{N}} = 33\text{ K}$ ^{21,23}. Existence of the SmIr_2Si_2 polymorphs has been confirmed by a structure study but information regarding magnetism is still

LaIr ₂ Si ₂	HTP $T_{SC}(K)$	LTP $T_{SC}(K)$
Ref ³¹	1.56	-
Ref ³²	1.52-1.58	-
Ref ³³	1.6	-
YIr ₂ Si ₂	HTP $T_{SC}(K)$	LTP $T_{SC}(K)$
Ref ³²	2.72-2.83	-
Ref ³⁴	2.6	2.6 (broaden)
Ref ³⁵	2.7	2.4
Ref ³⁶	2.7	2.45

Table I. The overview of the presence and temperatures of superconducting transitions in Y and La iridium silicides.

missing²⁴. As already mentioned EuIr₂Si₂ has been reported crystallizing only in the CaBe₂Ge₂ type structure and exhibits intermediate valence behavior^{15,24}. Rather incomplete information is available for the heavy rare-earth iridium silicides; for TmIr₂Si₂ no scientific data at all are available and for HoIr₂Si₂ besides confirmation of polymorphism²⁴ no other information has been published. The LTP of Gd, Tb, Dy and Er are reported to be antiferromagnetic below $T_N = 80, 80, 40$ and 10 K, respectively^{2,23-28}. Antiferromagnetism ($T_N = 13$ K) is reported also for the HTP of TbIr₂Si₂²⁵; no other physical properties of HTP are known for the heavy rare-earth iridium silicides except for the Yb compound. YbIr₂Si₂ attracted much interest owing to heavy fermion behavior of the LTP, which is close to a quantum critical point (QCP)^{25,26}. In contrary the HTP orders magnetically at 0.7 K^{25,27,28}. No information on physical properties of LuIr₂Si₂ has been published although the Lu compound was often mentioned as a non-magnetic analogue within the YbIr₂Si₂ study.

Superconductivity has been observed for the HTP of two REIr₂Si₂ compounds without the $4f$ electrons, namely YIr₂Si₂ and LaIr₂Si₂. The literature reports, which are briefly reviewed in Table I, are in some cases contradictory, especially as concerns presence of superconductivity in the LTP of YIr₂Si₂. In this context we would like to note that lanthanum at ambient pressure becomes a superconductor below about 6 K in both the h.c.p and f.c.c. crystal form, respectively in ambient pressure²⁹. In contrary yttrium metal under ambient pressure shows no superconductivity but Wittig³⁰ has discovered superconductivity in yttrium metal at 1.2 K when applying pressure of 11 GPa.

The primary objective of the present paper is to clarify how magnetism and superconductivity in YIr₂Si₂ and LaIr₂Si₂ is connected with the specific layered crystal structures of the two polymorphs (LTP and HTP). As a first step we studied existence of the LTP- and HTP-phase, respectively, with respect to thermal history by combining the DTA measurements with X-ray powder diffraction analysis of samples at room temperature. The main part of the paper is devoted to the low temperature measurements of the electrical resistivity, magnetization,

AC susceptibility and specific heat in various magnetic fields. To corroborate our explanation of experimental results we have also performed *ab initio* electronic structure calculations for YIr₂Si₂ and theoretical predictions regarding the superconducting state.

II. EXPERIMENTAL AND COMPUTATION DETAILS

In order to avoid problems with stabilizing the HTP at low temperatures when growing the single crystals by Czochralski method²³ we have decided to perform the work on polycrystals which can be easier quenched after melting and single-HTP samples can be obtained. The samples of YIr₂Si₂ and LaIr₂Si₂ compounds have been prepared by melting the stoichiometric amounts of elements (purity of Y and La - 99.9% , Ir - 99.99% , Si - 99.9999%) in an arc-furnace with a water-cooled copper crucible under the high-purity ($6N$) argon protective atmosphere. The total sample mass was typically 2.5 g. The samples were re-melted three times to ensure good homogeneity; finally the sample has been left to cool rapidly after sudden switching off the arc above the melt. No significant evaporation has been observed during melting the samples. Each sample has been cut into two equal parts. One half of the each sample was wrapped in a tantalum foil (99.9%), sealed in a quartz tube under the vacuum of $1 \cdot 10^{-6}$ mbar, annealed at 900°C for 7 days and then slowly cooled to avoid internal stresses. The second half was kept without any heat treatment. Both the samples (as cast and annealed) were characterized by the X-ray powder diffraction method (XRPD) at room temperature using a Bruker D8 Advance diffractometer equipped with a monochromator providing the $\text{CuK}\alpha$ radiation. The diffraction patterns were evaluated by the standard Rietveld technique³⁷ using the FullProf/WinPlotr software³⁸. The composition of samples was verified by chemical analysis using a scanning electron microscope (SEM) Tescan Mira I LMH equipped by an energy dispersive X-ray detector (EDX) Bruker AXS. The samples have been shaped appropriate for individual measurements using a fine wire saw to prevent additional stresses in the samples.

Differential thermal analysis (DTA) measurements were performed using Setaram SETSYS-2400 CS instrument over the range from room temperature to 1450°C . The heating and cooling rates were 5 K/min.

The low temperature behavior was tested by the electrical resistivity, heat capacity, magnetization and AC susceptibility measurements in the PPMS9T and MPMS7T facilities (Quantum Design). The samples for the electrical resistivity measurement were of the bar shape (1 mm x 1 mm x 4 mm). The electrical resistivity was measured as a function of temperature and magnetic field by using the four-terminal AC method. The heat capacity was measured on the 1.5 mm x 1.5 mm x 0.5 mm plates by the relaxation method. The magnetic measure-

ments were performed with fine powder samples having the grains fixed in random orientation by weakly magnetic glue. The electrical resistivity was measured also with a ^3He option down to the temperature of 350 mK³⁹.

The results of calculations of the electronic structure of LaIr_2Si_2 have been published before²². The ground-state electronic structure YIr_2Si_2 was calculated on the basis of DFT within the local spin density approximation (LSDA)⁴⁰ and the generalized gradient (GGA) approximation^{41–43} therefore we used more possibilities than just GGA⁴² in the work⁴⁴. For this purpose, we used the full-potential augmented-plane-wave plus local-orbitals method (APW-lo) as implemented in the latest version (WIEN2k) of the original WIEN code⁴⁵. The calculations were performed within scalar relativistic mode with the following parameters. Non-overlapping atomic-sphere (AS) radii of 2.8, 2.3 and 1.6 a.u. (1 a.u. = 52.9177 pm) were taken for Y, Ir and Si, respectively. The basis for the expansion of the valence states (less than 8 Ry below the Fermi energy) consisted of more than 3500 basis functions (more than 350 APW/atom) for the HTP-structure and more than 1350 (more than 270 APW/atom) for the LTP-structure plus the Y 3s, 3p, Ir 5s, 5p, 4f and Si 2p local orbitals. The Brillouin-zone integrations were performed with the tetrahedron method 47, on a 330 k-point mesh (HTP) and 288 (LTP) corresponding to more than 4000 k-points in the full Brillouin zone for both the crystal structures.

III. RESULTS AND DISCUSSION

A. Composition and crystal structure analysis

We have successfully synthesized the polycrystalline samples of the YIr_2Si_2 and LaIr_2Si_2 compounds and performed FE-EDX analysis at various locations of the annealed samples. The element analysis confirmed the majority of the YIr_2Si_2 and LaIr_2Si_2 phases, respectively, in all surveyed samples and 1-2 percent of the La rich and Si poor phase ($\text{La}_{1.04}\text{Ir}_2\text{Si}_{1.58}$) localized mainly on grain boundaries of the La based samples.

Subsequently, small pieces of the as-cast and annealed samples of both compounds, were powdered in agate mortar and XRPD data have been collected. We have observed significant difference between the patterns of the as-cast and annealed samples in the case of both compounds due to the crystal structure transformation within the thermal treatment. All reflections can be assigned to the ThCr_2Si_2 -type structure type in the case on thermally treated samples while the as-cast samples kept the CaBa_2Ge_2 -structure type. No significant additional reflections have been found in either sample. The powder patterns of the both compounds in the as-cast and annealed states are displayed in Figure 1.

The proper analysis of the XRPD pattern of the YIr_2Si_2 HTP revealed a mixture between the Si and Ir atoms in the $2c$ positions. The refinement process showed

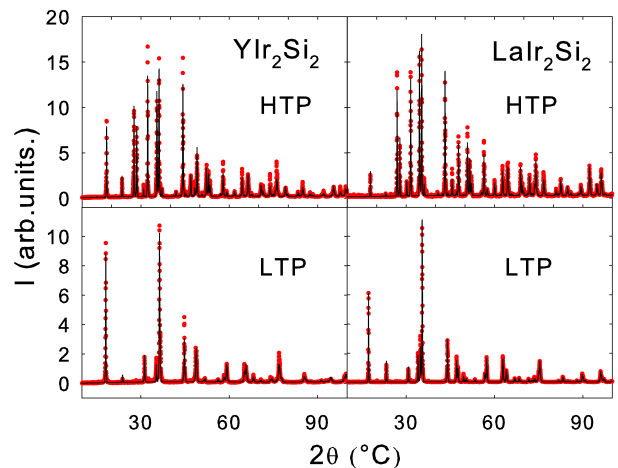


Figure 1. XRPD patterns of the YIr_2Si_2 and LaIr_2Si_2 compounds. The upper panels represent the patterns of the as-cast samples. The lower panels represent the patterns of the annealed materials as described in the text.

YIr ₂ Si ₂ – HTP		<i>a</i> (Å) 4.0938(2)		
CaBa ₂ Ge ₂ structure type		<i>c</i> (Å) 9.6856(7)		
Atoms	Symmetry	x	y	z
Ir	2 <i>c</i>	$\frac{1}{4}$	$\frac{1}{4}$	0.127(5)
Si	2 <i>c</i>	$\frac{1}{4}$	$\frac{1}{4}$	0.422(9)
Y	2 <i>c</i>	$\frac{1}{4}$	$\frac{1}{4}$	0.742(8)
Ir	2 <i>b</i>	$\frac{3}{4}$	$\frac{1}{4}$	$\frac{1}{2}$
Si	2 <i>a</i>	$\frac{3}{4}$	$\frac{1}{4}$	0

Table II. Crystal structure parameters of the HTP of YIr_2Si_2 .

mixture of about 10 – 12 %. A similar situation has been observed in the case of LaIr_2Si_2 with the Si/Ir mixture of about 5 %. On the other hand no atoms mixture has been detected in the LTP and all atoms of the involved elements well occupied their positions in both compounds. The crystal structure parameters of the YIr_2Si_2 compound are digestedly summarized in the Table II and Table III. The determined parameters are in good agreement with the structure model published by Shelton et al.³².

Lattice parameters and fractional coordinates of the

YIr ₂ Si ₂ – LTP		<i>a</i> (Å) 4.0483(2)		
ThCr ₂ Si ₂ structure type		<i>c</i> (Å) 9.8152(7)		
Atoms	Symmetry	x	y	z
Si	4e	0	0	0.3640(9)
Ir	4d	0	$\frac{1}{2}$	$\frac{1}{4}$
Y	2a	0	0	0

Table III. Crystal structure parameters of the LTP of YIr_2Si_2 .

LaIr ₂ Si ₂ – HTP		a (Å)	4.1873(1)	
CaBa ₂ Ge ₂ structure type		c (Å)	9.9380(3)	
Atoms	Symmetry	x	y	z
Ir	2c	$\frac{1}{4}$	$\frac{1}{4}$	0.374(4)
Si	2c	$\frac{1}{4}$	$\frac{1}{4}$	0.140(8)
La	2c	$\frac{1}{4}$	$\frac{1}{4}$	0.742(8)
Ir	2a	$\frac{3}{4}$	$\frac{1}{4}$	0
Si	2b	$\frac{3}{4}$	$\frac{1}{4}$	$\frac{1}{2}$

Table IV. Crystal structure parameters of the HTP of LaIr₂Si₂.

LaIr ₂ Si ₂ – LTP		a (Å)	4.1111(1)	
ThCr ₂ Si ₂ structure type		c (Å)	10.3001(3)	
Atoms	Symmetry	x	y	z
Si	4e	0	0	0.366(1)
Ir	4d	0	$\frac{1}{2}$	$\frac{1}{4}$
La	2a	0	0	0

Table V. Crystal structure parameters of the LTP of LaIr₂Si₂.

both LaIr₂Si₂ polymorphs are summarized in the Table IV and Table V.

The difference between corresponding lattice parameters of LaIr₂Si₂ and YIr₂Si₂ compounds is about 1 % which well corresponds with the difference between the La and Y atomic radii. The c/a ratio of HTP is 1% and 3% larger than the value for the LTP of YIr₂Si₂ and LaIr₂Si₂, respectively.

The transformation temperatures between the HTP and LTP in both compounds were studied by DTA and the typical result for the YIr₂Si₂ compound is displayed in Figure 2. Two thermal cycles have been applied on the as cast samples, which contain entirely the HTP. Two anomalies appeared in the first heating branch of the both compounds. When heating from room temperature the first anomaly corresponds with the transformation from the HTP, which is metastable at room temperature to the thermodynamically preferable LTP. The transformation temperature has been found $\sim 365^\circ\text{C}$ (651°C) for the LaIr₂Si₂ (YIr₂Si₂) compound. It is in good agreement with transition temperature 340°C for LaIr₂Si₂ compound reported by Mihalik et al.⁴⁶. The second anomaly appears when the LTP transforms to the HTP at 1101°C for LaIr₂Si₂ ($\sim 1140^\circ\text{C}$ by Mihalik et al.⁴⁶) and 1162°C for YIr₂Si₂. Only one transition has been found on the cooling branch, which corresponds to the reverse transition from the HTP to the LTP at 800°C for the LaIr₂Si₂ ($\sim 860^\circ\text{C}$ by Mihalik et al.⁴⁶) and 1013°C for the YIr₂Si₂ compound (see Figure 2).

In the case of YIr₂Si₂ the sample after the first thermal cycle can be considered as being in the well-annealed state, i.e. containing only the LTP. Therefore the 651°C anomaly is obviously missing on the heating branch of the second thermal cycle whereas the other features well

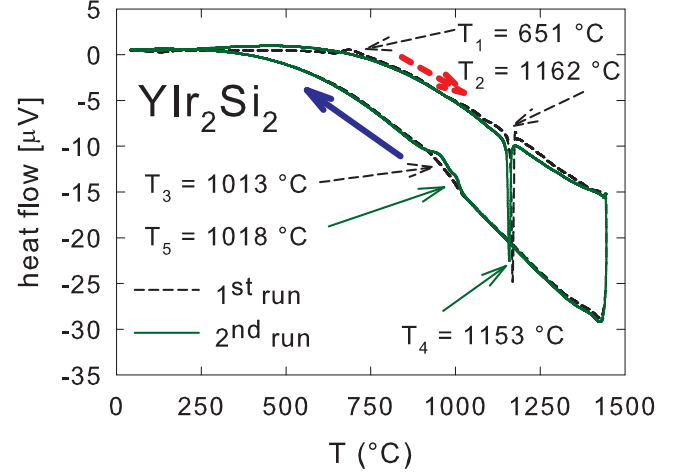


Figure 2. DTA curves recorded for YIr₂Si₂. The upper red bold (dashed) arrow denotes the heating branch. The lower blue bold (solid) arrow denotes the cooling branch. Temperatures of transitions are numbered and marked by black (dashed) arrows for first run and green (solid) arrow for second run.

Transf. T (°C)	YIr ₂ Si ₂	LaIr ₂ Si ₂	LaIr ₂ Si ₂ ⁴⁶
T_1	651	365	340
T_2	1162	1101	1140
T_3	1013	800	860
T_4	1153	1107	not measured
T_5	1018	-	not measured
$ T_2 - T_3 $	149	301	not measured

Table VI. List of transition temperatures for all compounds, First run: T_1 - temperature of the transformation of the metastable (at room temperature) HTP to stable LTP, T_2 - temperature of the transition from the stable LTP to the stable HTP, T_3 - temperature of the transition from the stable HTP to the stable LTP; second run: T_4 - temperature of the transition from the stable LTP to the stable HTP, T_5 - temperature of the transition from the stable HTP to the stable LTP, $|T_2 - T_3|$ represents thermal hysteresis of HTP-LTP transformation in the 1st run.

correspond to these observed in the first thermal cycle.

The observed transformation temperatures are digested and summarized in the Table VI.

To achieve the desirable YIr₂Si₂ and LaIr₂Si₂ samples for measurements of low temperature properties which contain entirely the LPT we annealed the as cast samples in the temperature interval $800 - 900^\circ\text{C}$ (which is high enough to transform the frozen HTP to the LTP but low enough to prevent the LTP to the HTP transformation). The cooling rate used after annealing was lower than 1 K/min. Then the annealed samples have been found free of any traces of HTP.

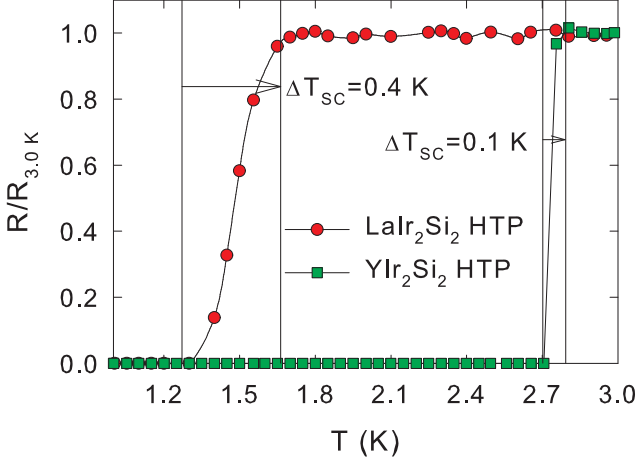


Figure 3. Temperature dependence of the electrical resistivity for the LaIr_2Si_2 HTP and YIr_2Si_2 HTP. The sharp drop of resistivity signs the superconductivity transition.

B. Resistivity and heat capacity results

We have measured electrical resistivity data of the as-cast (HTP) and annealed (LTP) samples of both compounds and we have observed significantly different behavior. While the HTP of both compounds, respectively, exhibit robust superconductivity – see the drop of the resistivity around the superconducting transition temperature T_{SC} , which has been assigned to the maximum slope of the resistivity drop (Figure 3). We have found the values of $T_{\text{SC}} = 2.72$ K for YIr_2Si_2 and $T_{\text{SC}} = 1.4$ K for LaIr_2Si_2 . Nevertheless there is a significant difference between the SC transition of the La and Y compound. While a very sharp transition from normal to superconducting state within 0.1 K has been detected for the Y compound a broader transition (0.4 K) occurs in the La compound (see Figure 3). The relatively high temperatures of the superconducting transition in HTP (higher than 1 K) are attributed to the unique arrangement of the Ir atoms in the 5 Si pyramidal cages in the HTP crystal structure. It is therefore tempting to speculate that the transition-metals coordination in these silicides is linked with and may be crucial for the occurrence of superconductivity in these compounds³³, which may happen if the material is not well annealed. No sign of superconductivity has been detected in the LTP polymorphs down to the lowest temperature of our experiment (0.4 K). It is in contradiction with some previous papers where superconductivity in YIr_2Si_2 was reported for both the HTP and LTP samples^{34,36}. We believe that the main reason of superconductivity observed in the LTP samples reported in some earlier papers can be attributed to the presence of certain amount of the HTP in these samples.

To confirm the bulk superconducting properties we have measured the heat capacity data of all four samples and have observed also here significantly different

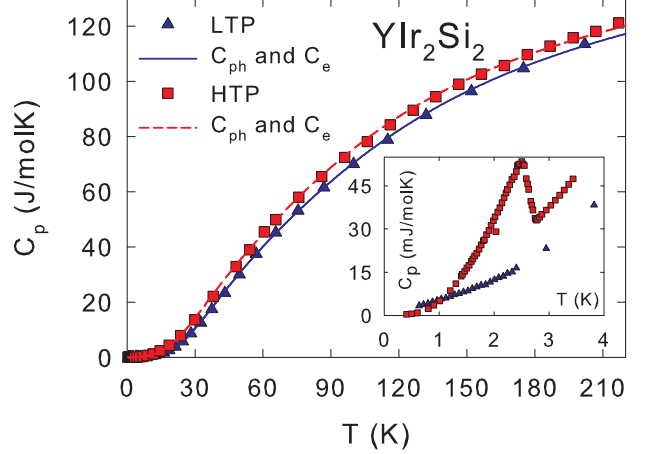


Figure 4. Temperature dependence of heat capacity of the YIr_2Si_2 sample. The marks represent measured data where every second point has been omitted for clarity. The lines correspond to the fitted models.

behavior of the HTP and LTP samples of corresponding compounds similar to resistivity behaviour. While the HTP of both compounds were superconducting – see the anomaly at temperatures of the superconducting transitions in the heat capacity data (Figure 4 and Figure 5) no sign of any transition has been observed in the data of the LTPs. The T_{SC} values determined from the heat capacity behavior are somewhat lower than these indicated by resistivity data. We have found the critical values based on heat capacity data of $T_{\text{SC}} = 2.52$ K for the YIr_2Si_2 and $T_{\text{SC}} = 1.24$ K for the LaIr_2Si_2 compound. The T_{SC} values of the both HTP of both compounds well correspond with values found for HTP in literature which are listed in the Table I.

We have analyzed the heat capacity considering it as a sum of electron (C_e) and phonon (C_{ph}) contribution:

$$C_e = \frac{2\pi^2 k_B^2 T}{E_F} = \gamma T \quad (1)$$

where n is the density of electronic states at Fermi level E_F and k_B is Boltzmann constant.

The phonon contribution was treated within the Debye and Einstein models using anharmonicity correction⁴⁷. The values of the Debye and Einstein temperatures and degeneracy of the Einstein modes are listed in Table VII and Table VIII.

Values of the Sommerfeld γ coefficient determined from the specific heat data are summarized in Table IX.

Our experimental values of γ coefficient can compare as well with the coefficients presented by Braun et al.³¹. The value of $\gamma = 8.5 \text{ mJ} \cdot \text{mol}^{-1} \cdot \text{K}^{-2}$ presented by Braun et al. for HTP is in good agreement with our observed value. On the other hand our experimental value of γ is significantly higher than the value

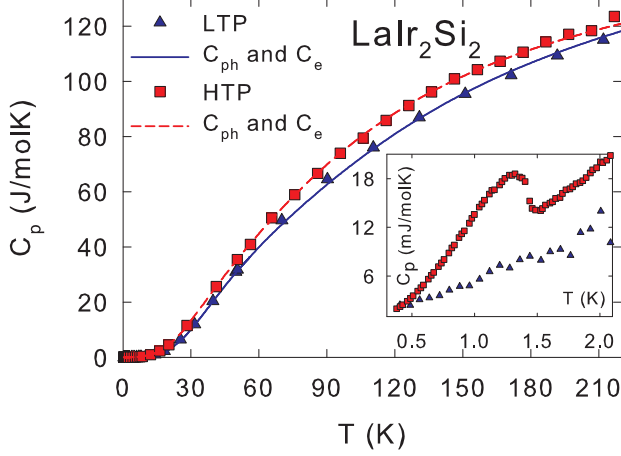


Figure 5. Temperature dependence of heat capacity of the LaIr_2Si_2 sample. The marks represent measured data where every second point has been omitted for clarity. The lines correspond to the fitted models.

YIr_2Si_2		HTP			LTP		
Branch	Degen.	$\theta[\text{K}]$	$\alpha \cdot 10^{-4} [\text{K}^{-1}]$		Degen.	$\theta[\text{K}]$	$\alpha \cdot 10^{-4} [\text{K}^{-1}]$
θ_D		145				180	4
θ_{E1}	2	170	4		2	180	4
θ_{E2}	3	180	4		3	185	4
θ_{E3}	3	405	4		3	390	4
θ_{E4}	4	410	4		4	395	4

Table VII. Phonon spectrum of the both polymorphs of the YIr_2Si_2 compound.

LaIr_2Si_2		HTP			LTP		
Branch	Degen.	$\theta[\text{K}]$	$\alpha \cdot 10^{-4} [\text{K}^{-1}]$		Degen.	$\theta[\text{K}]$	$\alpha \cdot 10^{-4} [\text{K}^{-1}]$
θ_D		155				200	5
θ_{E1}	2	170	4		2	170	5
θ_{E2}	3	175	4		3	175	5
θ_{E3}	3	390	4		3	470	5
θ_{E4}	4	395	4		4	475	5

Table VIII. Phonon spectrum of the both polymorphs of the LaIr_2Si_2 compound.

	YIr_2Si_2		LaIr_2Si_2	
	HTP	LTP	HTP	LTP
$\gamma [\text{mJ} \cdot \text{mol}^{-1} \cdot \text{K}^{-2}]$	8	8	8.1	8.1

Table IX. Sommerfeld γ coefficient of all compounds.

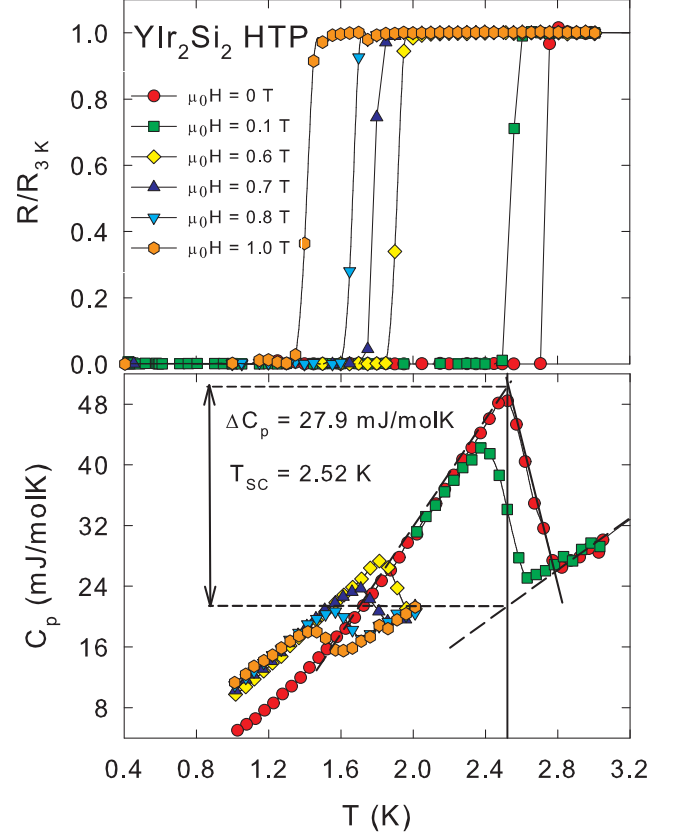


Figure 6. Temperature dependence of the specific heat and electric resistivity of the HTP of YIr_2Si_2 measured in various magnetic fields.

$\gamma = 4.5 \text{ mJ} \cdot \text{mol}^{-1} \cdot \text{K}^{-2}$ presented by Braun et al.³¹ for the LTP.

In order to analyze the superconducting properties of both compounds with respect to the predictions of BCS theory we have measured the heat capacity and electrical resistivity at low temperatures under various magnetic fields. The results are shown in Figure 6 and 7 for HTPs of YIr_2Si_2 and LaIr_2Si_2 , respectively, which were found superconducting. Only curves in selected magnetic fields are displayed from the heat capacity measurements for better clarity. It is also important to note that we have always found a sharp drop of resistivity at the SC transition for all the applied magnetic fields for the YIr_2Si_2 . The broadened transitions were observed for LaIr_2Si_2 both in zero magnetic field ($\Delta T = 0.4 \text{ K}$) and also under the applied magnetic field when two step like transitions developed.

We have plotted all the values of the critical fields from all used methods and their temperature evolution for both YIr_2Si_2 and LaIr_2Si_2 in the Figure 8 and Figure 9. In the case of YIr_2Si_2 we have found good agreement between the temperature evolution between the resistivity and heat capacity data. Only the AC susceptibility data measured for a narrow temperature interval (2.6-2.1

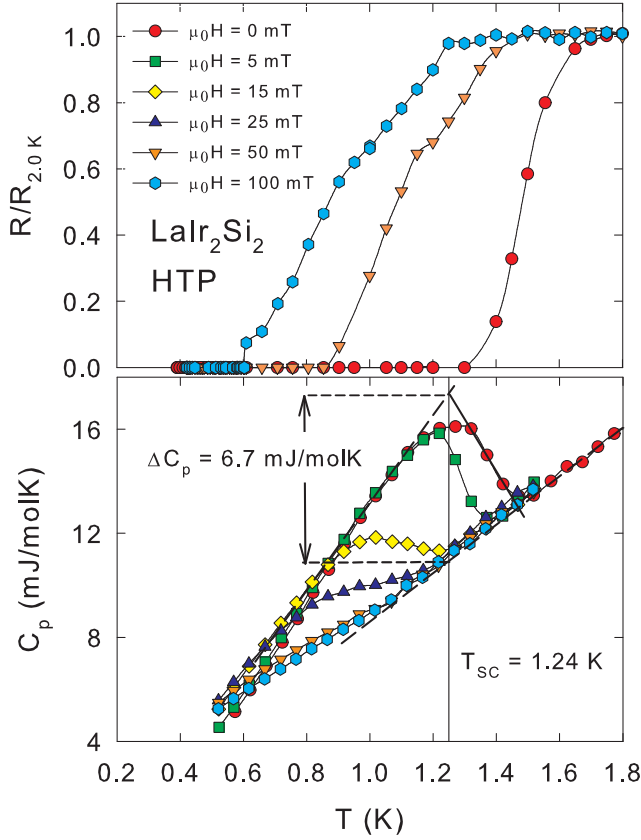


Figure 7. Temperature dependence of the specific heat and electric resistivity of the HTP of LaIr_2Si_2 measured in various magnetic fields.

K) are slightly shifted to lower fields. First we have tested to evaluate the temperature evolution of the critical field using the square law (Equation (2)) .

$$\mu_0 H_{C2}(T) = \mu_0 H_{C2}(0) \left[1 - (T/T_{SC})^2 \right] \quad (2)$$

The square law was not found as a reasonable model for significant undervalue of the $\mu_0 H_{C2}(0)$ parameter in the case of YIr_2Si_2 . The value of $\mu_0 H_{C2}(0)$ was found to be 1.27 T using square law. We have obtained more satisfying results using formula derived from Ginzburg-Landau theory⁴⁸⁻⁵⁰ (Equation (3)).

$$\mu_0 H_{C2}(T) = \mu_0 H_{C2}(0) \left[\frac{1 - (T/T_{SC})^2}{1 + (T/T_{SC})^2} \right] \quad (3)$$

This formula gives $\mu_0 H_{C2}(0) = 1.67$ T as a result of the explanation of the resistivity data and similar value $\mu_0 H_{C2}(0) = 1.72$ T for the heat capacity data. The value of the critical field for LaIr_2Si_2 compound have been also unsuccessfully approximated by the square law (Equation (2)) that gives the value of the critical field $\mu_0 H_{C2}(0) =$

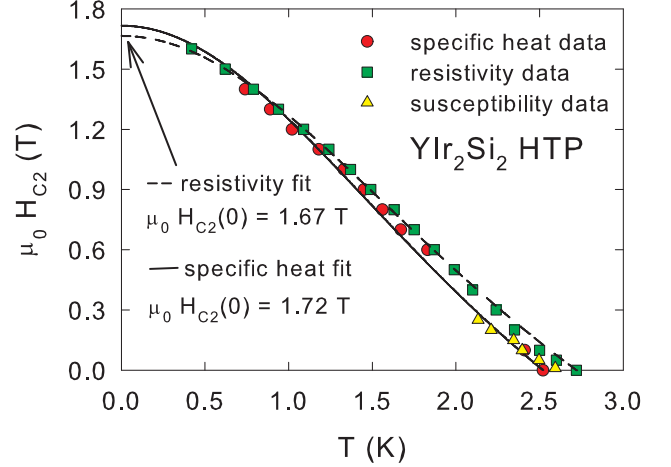


Figure 8. Temperature dependence of the critical fields of the YIr_2Si_2 HTP. Measured data are fitted using Equation (3).

42.1 mT when applied on the heat capacity data. Also in this case Ginzburg-Landau formula (Equation (3)) gives better results and estimates the value of the critical field $\mu_0 H_{C2}(0) = 56.2$ mT for the heat capacity data. Fitting of the resistivity data gives significantly a higher value of the critical field $\mu_0 H_{C2}(0) = 137.2$ mT. Such behavior unambiguously denoted that the LaIr_2Si_2 sample was not in full bulk superconducting state as it will be also later confirmed by anomaly low value of the $(\Delta C_p)_{T_{SC}}/\gamma T_{SC}$.

On the basis of these findings we have tried to estimate the value of the $\mu_0 H_{C2}(0)$ from the specific heat data using Werthamer-Helfand-Hohenberg (WHH) formula (Equation (4))⁵¹ within the weak-coupling BCS theory, as well.

$$\mu_0 H_{C2}(0) = -0.693 (dH_{C2}/dT_{SC}) T_{SC} \quad (4)$$

We have approximated the value of the critical field $\mu_0 H_{C2}(0) \approx 1.6$ T YIr_2Si_2 and only ≈ 40 mT for LaIr_2Si_2 . Mainly the WHH value of $\mu_0 H_{C2}(0)$ is in very good experimental agreement in the case of the Y compound. All the $\mu_0 H_{C2}(0)$ values are also digestedly compared and summarized in the Table XII.

The specific heat jump at temperature $T_{SC} = 2.52$ K in zero magnetic field reaches the value $\Delta C_p = 27.9 \text{ mJ} \cdot \text{mol}^{-1} \cdot \text{K}^{-1}$ in the case of YIr_2Si_2 while significantly lower and broadened jump of $\Delta C_p = 6.7 \text{ mJ} \cdot \text{mol}^{-1} \cdot \text{K}^{-1}$ occurred for LaIr_2Si_2 . We have tried to estimate the value of the $(\Delta C_p)_{T_{SC}}/\gamma T_{SC}$, which should be 1.43 based on BSC weak-coupling theory. The value of 1.38 obtained for YIr_2Si_2 , in good agreement with the predicted value of 1.43. Contrary to that the corresponding value for the LaIr_2Si_2 is significantly lower than expected - only 0.67. As we have mentioned hereinbefore we presume that the sample did not reach the superconducting state at a certain sharp temperature inter-

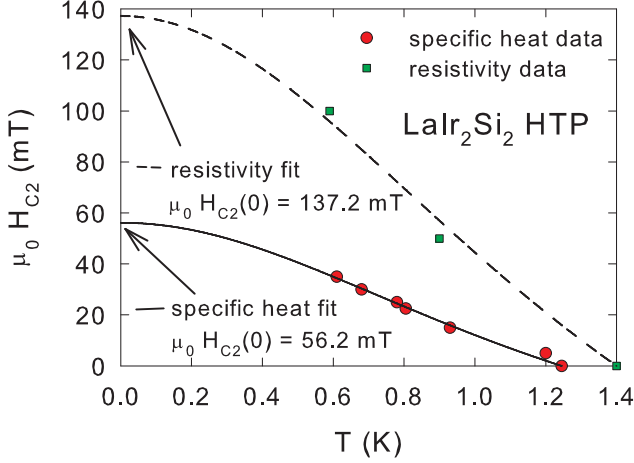


Figure 9. Temperature dependence of the critical field of the LaIr_2Si_2 HTP. Measured data are fitted using Equation (3).

val because of broadening of the superconducting transition probably due to mechanical stresses. Moreover only part of the sample was superconducting. Similar situation can occur in intermetallics as was found for example in Ref.⁵² because standard BCS behavior of the La compound was found in Ref.³¹ with $(\Delta C_P)_{T_{SC}}/\gamma T_{SC} = 1.3$ which is 90 % of the BCS-predicted value.

C. First principles electronic structure calculations

The first principles calculations started minimizing the forces at the symmetry free Wyckoff positions for both HTP and LTP structures. We have found very good agreement with our experimental data. Using fixed spin moment method it has been confirmed Pauli paramagnet as the ground state of the YIr_2Si_2 for both the HTP and LTP.

We now compare the performance of LSDA and GGA with respect to the equilibrium volume of the HTP and LTP. The ratio c/a has been also minimized and found to be close to the experimental equilibrium (see Table X and XI). We have calculated the variation of the total energy with the relative volume V/V_0 (V_0 is the experimental equilibrium volume). The LSDA⁴⁰ value of the equilibrium volume is less than 1.0 % smaller than the experimental value. The GGA from Ref.⁴², on the other hand, leads to a volume that exceeds the experimental V_0 by 3.8 % and the volume obtained with the GGA from Ref.⁴¹ is 1.3 % larger. The best results are obtained using the GGA from Ref.⁴³, which underestimates V_0 by only 1.1%. An all forms of the GGA^{41–43} provide a worse equilibrium volume than the LSDA. Finally we have calculated the structural difference energy using LSDA. We have found the value 9 mRy per formula unit and the LT phase is lower in energy with agreement to our experimental data.

	YIr_2Si_2		reference
	LTP	HTP	
$(c/a)_{\text{theor}}$	2.4474	2.3791	this work
$(c/a)_{\text{exp}}$	2.4245	2.3659	this work
	LaIr_2Si_2		
	LTP	HTP	
$(c/a)_{\text{theor}}$	2.5070	2.3749	Ref. ²²
$(c/a)_{\text{exp}}$	2.5054	2.3734	this work

Table X. c/a ratios as a result of DFT calculations in comparison with measured data.

YIr_2Si_2 - LTP - experimental data							calculated values
Atom	Symmetry	x	y	z	x	y	z
Si	4e	0	0	0.36409	0	0	0.37934
Ir	4d	0	0.5	0.25	0	0.5	0.25
Y	2a	0	0	0	0	0	0
YIr_2Si_2 - HTP - experimental data							calculated values
Atom	Symmetry	x	y	z	x	y	z
Ir	2c	0.25	0.25	0.12753	0.25	0.25	0.12822
Si	2c	0.25	0.25	0.42296	0.25	0.25	0.36808
Y	2a	0.25	0.25	0.74891	0.25	0.25	0.7538
Ir	2b	0.75	0.25	0.5	0.75	0.25	0.5
Si	2c	0.75	0.25	0	0.75	0.25	0

Table XI. Atomic coordinates obtained from DFT calculations compared with measured values.

We have checked the calculated density of the electronic states and it is in perfect agreement with the results in Ref.⁴⁴. The DOS value at the Fermi level is $N(E_F) = 2.36$ states/eV f.u. and $N(E_F) = 2.05$ states/eV f.u. which correspond to $\gamma_{\text{band}} = 5.64 \text{ mJ} \cdot \text{mol}^{-1} \cdot \text{K}^{-2}$ and $\gamma_{\text{band}} = 4.9 \text{ mJ} \cdot \text{mol}^{-1} \cdot \text{K}^{-2}$ for the HTP and LTP, respectively. The experimental specific-heat value is $\gamma_{\text{exp}} = 8.0 \text{ mJ} \cdot \text{mol}^{-1} \cdot \text{K}^{-2}$ for the HTP, which points to an enhancement factor of $\lambda = 0.42$, λ being defined by $\gamma_{\text{exp}} = \gamma_{\text{band}}(1 + \lambda)$. This total enhancement is most likely due to the electron-phonon coupling.

The first superconducting temperature T_{SC} -relation based on the minimum set of three parameters (averaged Debye temperature θ_D , mass-enhancement coefficient λ and a Coulomb pseudopotential μ^*) which found extensive applications in the analysis of superconductors was worked out by McMillan⁵³. Starting with the full Eliashberg equations, McMillan introduced ad hoc assumptions on the nature of the spectral function and assumed further that T_{SC} depends on spectral function only through λ . Performing numerical solutions of the Eliashberg equations McMillan derived so-called McMillan-formula (Equation (5)).

$$T_{\text{SC}} = \frac{\theta_{\text{D}}}{1.45} \exp \left(-\frac{1.04(1+\lambda)}{\lambda - \mu^*(1+0.62\lambda)} \right) \quad (5)$$

Using the averaged Debye temperature $\theta_{\text{D}} = 145$ K, the mass-enhancement coefficient $\lambda = 0.42$ and the Coulomb pseudopotential $\mu^* = 0.13$ we have found $T_{\text{SC}} = 0.45$ K. This only semiquantitatively agrees with our experimental value $T_{\text{SC}} = 2.52$ K. We note that the result of using McMillan formula is especially very sensitive to particular value of mass-enhancement coefficient λ which is the result of combined analysis of experimental specific heat data and first-principles calculations based on the DFT with approximate exchange correlation functional. For example the value of $\lambda = 0.6$ $T_{\text{SC}} \sim 1$ K which is quite close to our experimental value $T_{\text{SC}} = 2.52$ K. We also point out that we used Coulomb pseudopotential $\mu^* = 0.13$ which is a common practice to follow suggestion of McMillan⁵³ for all transition metals and their compounds. Therefore our calculations using McMillan formula can be taken as a starting crude estimate of T_{SC} only. One possible reason of limiting validity of using of McMillan formula for our YIr_2Si_2 might be the complex nature of the phonon spectra in YIr_2Si_2 compound and therefore the coupling of electrons to special phonon modes. Therefore the full first-principles calculation of the superconducting temperature T_{SC} of YIr_2Si_2 is clearly beyond the scope of the present paper.

D. Magnetization data

The experimental magnetic susceptibility of YIr_2Si_2 in the normal state is temperature independent and the value is close to $2.5 \cdot 10^{-8} \text{ m}^3 \cdot \text{mol}^{-1}$ for HTP and $1.5 \cdot 10^{-8} \text{ m}^3 \cdot \text{mol}^{-1}$ for LTP, respectively. The theoretical value of $8.4 \cdot 10^{-8} \text{ m}^3 \cdot \text{mol}^{-1}$ for HTP and $7.3 \cdot 10^{-8} \text{ m}^3 \cdot \text{mol}^{-1}$ for LTP, respectively calculated by using the well-known equation for Pauli susceptibility (Equation (6)) provides only right order with the experimental value. The overestimation of the theoretical value is probably connected with approximate exchange correlation functional used in our first principles DFT calculations.

$$\chi = \mu_{\text{B}}^2 N(E_{\text{F}}) \quad (6)$$

IV. CONCLUSIONS

We have successfully verified, that polymorphism is an effective tool to study the influence of the crystal symmetry as a deciding parameter for presence of the superconductivity on materials. As a model example we have successfully synthesized both tetragonal polymorphs of the YIr_2Si_2 and LaIr_2Si_2 compounds, respectively. We

parameter	YIr_2Si_2 HTP	LaIr_2Si_2 HTP	YIr_2Si_2 LTP	LaIr_2Si_2 LTP
$T_{\text{SC}} C_{\text{P}}$ (K)	2.52	1.24	No SC	No SC
$T_{\text{SC}} R$ (K)	2.72K	1.45	No SC	No SC
$T_{\text{SC}} A C \chi$ (K)	2.7 – 2.2	-	No SC	No SC
$T_{\text{SC}}^{\text{theor.}}$ (K)	0.45	-	-	-
χ_{exp} ($10^{-8} \text{ m}^3 \cdot \text{mol}^{-1}$)	2.5	-	1.5	1.8
χ_{theor} ($10^{-8} \text{ m}^3 \cdot \text{mol}^{-1}$)	8.4	-	7.3	-
$\mu_0 H_{C2}(0)$ WHH (T)	1.59	0.041	-	-
$\mu_0 H_{C2}(0)$ sq.law (T)	1.27	0.042	-	-
$\mu_0 H_{C2}(0)$ GL – HC (T)	1.72	0.056	-	-
$\mu_0 H_{C2}(0)$ GL – R (T)	1.67	0.137	-	-
γ_{exp} ($\text{mJ} \cdot \text{mol}^{-1} \cdot \text{K}^{-2}$)	8	8	8.1	8.1
γ_{theor} ($\text{mJ} \cdot \text{mol}^{-1} \cdot \text{K}^{-2}$)	5.6	-	4.9	-
$\xi(0)$ GL (nm)	509	88.4	-	-
$\xi(0)$ WHH (nm)	455	89.7	-	-
$\Delta C / \gamma T_{\text{SC}}$	1.38	0.67	-	-
θ_{D} (K)	145	155	180	200
λ	0.42	-	-	-
$(c/a)_{\text{theor}}$	2.3791	2.3749 ²²	2.4474	2.5070 ²²
$(c/a)_{\text{exp}}$	2.3659	2.3734	2.4245	2.5054

Table XII. List of the parameters of the polymorphs of YIr_2Si_2 and LaIr_2Si_2 .

have determined the role of thermal treatment in formation of the LTP and the metastable HTP in detail. We conclude that not only the maximum temperature but also the cooling rate have been found as crucial parameters to obtain the single-phase material which can explain the controversial reports on the existence of the superconductivity in *122* iridium silicides presented in previous works. We have confirmed that only the HTP is superconducting; $T_{\text{SC}} = 2.52$ K and 1.24 K for YIr_2Si_2 and LaIr_2Si_2 , respectively. The LTP of both, YIr_2Si_2 and LaIr_2Si_2 , behave as the normal metallic conductors (no sign of superconductivity). The presence of the superconductivity in Y and La iridium silicides is connected with unique inverse stacking of Ir-Si layers in the HTP structure creating pyramidal Ir cages with La or Y atoms inside, which are not present in LTP polymorphs.

To well understand more physics of the *122* iridium silicides we have determined all the structure parameters, electronic structure and we have also inspected the superconducting state of both superconducting compounds within the BCS theory predictions.

The lattice parameters and atoms fractional coordinates were found to be in good agreement with previously published structure models^{32,33} and also in agreement with our theoretical DFT values obtained using GGA. The LT polymorphs have been also confirmed being thermodynamically favorable at room temperature. The low values of the coefficient $\gamma = 8.1 \text{ mJ} \cdot \text{mol}^{-1} \cdot \text{K}^{-2}$ for the YIr_2Si_2 and $\gamma = 8.0 \text{ mJ} \cdot \text{mol}^{-1} \cdot \text{K}^{-2}$ for the LaIr_2Si_2 of the HT polymorph denotes the low density of states at Fermi level, which was confirmed by theoretical calculations. We have also revealed a low mass enhancement ($\lambda = 0.42$) for the YIr_2Si_2 , which indicates a weak

electron-phonon interaction. According to the straightforward use of McMillan formula the theoretical value of the superconducting temperature is 0.45 K which is not so bad results in comparison to other Y intermetallics. Therefore we tentatively propose that the observed superconductivity might for example result from the coupling of electrons to special phonon modes in the Y and La iridium silicides complex phonon spectra. All physical parameters and found constants for the YIr_2Si_2 and LaIr_2Si_2 are digestedly summarized in the table XII.

ACKNOWLEDGMENTS

The work is a part of activities of the Charles University Research Center "Physics of Condensed Matter and Functional Materials. It was also supported by the Czech Science Foundation (Project # 202/09/1027) and the Charles University Grant Agency Project # 719612.

- ¹ L. Chelmicki, J. Leciejewicz, and A. Zygmunt, *Journal of Physics and Chemistry of Solids* **46**, 529 (1985).
- ² G. Czjzek, V. Oestreich, H. Schmidt, K. Laka, and K. Tomala, *Journal of Magnetism and Magnetic Materials* **79**, 42 (2004).
- ³ M. W. Dirken, R. C. Thiel, and K. H. J. Buschow, *Journal of The Less-Common Metals* **147**, 97 (1989).
- ⁴ E. H. E. Ghadraoui, J. Y. Pivan, R. Guqrin, O. Pena, J. Padiou, and M. Sergent, *Materials Research Bulletin* **23**, 1345 (1988).
- ⁵ I. Felner and I. Nowik, *Solid State Communications* **47**, 831 (1983).
- ⁶ I. Felner and I. Nowik, *Journal of Physics and Chemistry of Solids* **45**, 419 (1984).
- ⁷ I. Felner and I. Nowik, *Journal of Physics and Chemistry of Solids* **46**, 681 (1985).
- ⁸ H. Fujii and A. Sato, *Journal of Alloys and Compounds* **487**, 198 (2009).
- ⁹ K. Hiebl and P. Rogl, *Journal of Magnetism and Magnetic Materials* **50**, 39 (1985).
- ¹⁰ W. Jeitschko and M. Reehuis, *Journal of Physics and Chemistry of Solids* **48**, 667 (1987).
- ¹¹ W. Jeitschko, R. Glaum, and L. Boonk, *Journal of Solid State Chemistry* **69**, 93 (1987).
- ¹² M. Kuznietz, H. Pinto, H. Ettegui, and M. Melamud, *Phys Rev B* **40**, 7328 (1989).
- ¹³ J. Leciejewicz, ceiling left, M. Slaski, and A. Zygmunt, *Solid State Communications* **52**, 475 (1984).
- ¹⁴ S. Quezel, J. Rossatmignod, B. Chevalier, P. Lejay, and J. Etourneau, *Solid State Communications* **49**, 685 (1984).
- ¹⁵ B. Chevalier, J. M. D. Coey, B. Lloret, and J. Etourneau, *Journal of Physics C-Solid State Physics* **19**, 4521 (1986).
- ¹⁶ B. Buffat, B. Chevalier, M. H. Tuilier, B. Lloret, and J. Etourneau, *Solid State Communications* **59**, 17 (1986).
- ¹⁷ M. Mihalik, M. Divis, and V. Sechovsky, *Physica B: Condensed Matter* **404**, 3191 (2009).
- ¹⁸ T. Endstra, G. J. Nieuwenhuys, A. A. Menovsky, and J. A. Mydosh, *Journal of Applied Physics* **69**, 4816 (1991).
- ¹⁹ M. Mihalik, M. Divis, and V. Sechovsky, *Journal of Magnetism and Magnetic Materials* **322**, 1153 (2010).
- ²⁰ M. Mihalik, M. Divis, V. Sechovsky, N. Kozlova, J. Freudenberger, N. Stüser, and A. Hoser, *Phys Rev B* **81** (2010).
- ²¹ R. Welter, K. Halich, and B. Malaman, *Journal of Alloys and Compounds* **353**, 48 (2003).
- ²² M. Mihalik, Z. Matej, M. Divis, and V. Sechovsky, *Intermetallics* **17**, 927 (2009).
- ²³ M. Mihalik, J. Pospisil, A. Hoser, and V. Sechovsky, *Phys Rev B* **83** (2011).
- ²⁴ B. Chevalier, P. Lejay, B. Lloret, W. X. Zhong, J. Etourneau, and P. Hagenmuller, *Annales de Chimie-Science des Matériaux* **9**, 987 (1984).
- ²⁵ Z. Hossain, C. Geibel, T. Radu, Y. Tokiwa, F. Weickert, C. Krellner, H. Jeevan, P. Gegenwart, and F. Steglich, *Physica B-Condensed Matter* **378-80**, 74 (2006).
- ²⁶ S. Danzenbacher, Y. Kucherenko, C. Laubschat, D. V. Vyalikh, Z. Hossain, C. Geibel, X. J. Zhou, W. L. Yang, N. Mannella, Z. Hussain, Z. X. Shen, and S. L. Molodtsov, *Phys Rev Lett* **96** (2006).
- ²⁷ A. Hiess, O. Stockert, M. M. Koza, Z. Hossain, and C. Geibel, *Physica B: Condensed Matter* **378-380**, 748 (2006).
- ²⁸ Y. Tokiwa, P. Gegenwart, Z. Hossain, J. Ferstl, G. Sparr, C. Geibel, and F. Steglich, *Physica B-Condensed Matter* **378-80**, 746 (2006).
- ²⁹ W. T. Ziegler, R. A. Young, and A. L. Floyd, *J. Am. Chem. Soc.* **75**, 1215 (1953).
- ³⁰ J. Wittig, *Phys Rev Lett* **24**, 812 (1970).
- ³¹ H. F. Braun, T. Jarlborg, and A. Junod, *Physica B+C* **135**, 397 (1985).
- ³² R. N. Shelton, H. F. Braun, and E. Musick, *Solid State Communications* **52**, 797 (1984).
- ³³ H. F. Braun, N. Engel, and E. Parthé, *Phys Rev B* **28**, 1389 (1983).
- ³⁴ M. Hirjak, P. Lejay, B. Chevalier, J. Etourneau, and P. Hagenmuller, *Journal of the Less Common Metals* **105**, 139 (1985).
- ³⁵ I. Higashi, P. Lejay, B. Chevalier, J. Etourneau, and P. Hagenmuller, *Revue de Chimie Minérale* **21**, 239 (1984).
- ³⁶ P. Lejay, I. Higashi, B. Chevalier, M. Hirjak, J. Etourneau, and P. Hagenmuller, *Comptes Rendus de l'Académie des Sciences Serie II* **296**, 1583 (1983).
- ³⁷ H. M. Rietveld, *Journal of Applied Crystallography* **2**, 65 (1969).
- ³⁸ J. Rodríguez-Carvajal, *Physica B* **192**, 55 (1993).
- ³⁹ J. Prokleska, J. Pospisil, J. V. Poltirova, V. Sechovsky, and J. Sebek, *Journal of Physics: Conference Series* **200**, 012161 (2010).
- ⁴⁰ J. P. Perdew and Y. Wang, *Phys Rev B* **45**, 13244 (1992).
- ⁴¹ Z. G. Wu and R. E. Cohen, *Phys Rev B* **73**, 235116 (2006).
- ⁴² J. P. Perdew, K. Burke, and M. Ernzerhof, *Phys Rev Lett* **77**, 3865 (1996).
- ⁴³ J. P. Perdew, A. Ruzsinszky, G. I. Csonka, O. A. Vydrov, G. E. Scuseria, L. A. Constantin, X. Zhou, and K. Burke, *Phys Rev Lett* **100**, 136406 (2008).
- ⁴⁴ I. R. Shein, *Physica B: Condensed Matter* **406**, 3525 (2011).
- ⁴⁵ K. Schwarz, P. Blaha, and G. K. H. Madsen, *Computer*

- Physics Communications **147**, 71 (2002).
- ⁴⁶ M. Mihalik, J. Pospisil, A. Rudajevova, X. Marti, D. Wallacher, A. Hoser, T. Hofmann, M. Divis, and V. Sechovsky, *Intermetallics* **19**, 1622 (2011).
- ⁴⁷ C. A. Martin, *J Phys-Condens Mat* **3**, 5967 (1991).
- ⁴⁸ M. Tinkham, *Phys. Rev.* **129**, 2413 (1963).
- ⁴⁹ J. A. Woollam, R. B. Somoano, and P. O'Connor, *Phys Rev Lett* **32**, 712 (1974).
- ⁵⁰ A. Narduzzo, M. S. Grbic, M. Pozek, A. Dulcic, D. Paar, A. Kondrat, C. Hess, I. Hellmann, R. Klingeler, J. Werner, A. Kohler, G. Behr, and B. Buchner, *Phys Rev B* **78**, 012507 (2008).
- ⁵¹ N. R. Werthamer, E. Helfand, and P. C. Hohenberg, *Phys. Rev.* **147**, 295 (1966).
- ⁵² J. Pospisil, M. Kratochvilova, M. Divis, J. Prokleska, J. V. Poltierova, and S. V., *Journal of Alloys and Compounds* **509**, 1401 (2011).
- ⁵³ W. L. Mcmillan, *Phys. Rev.* **167**, 331 (1968).